Naphthyl thio- and carba-xylopyranosides for exploration of the active site of β4GalT7: The role of the endocyclic oxygen atom

Karin Thorsheim,[a] Daniel Willén,[a] Emil Tykesson,[a,b] Jonas Ståhle,[c] Jean-Pierre Praly,[d] Sébastien Vidal,[d] Magnus T. Johnson,[a] Göran Widmalm,[c] Sophie Manner.[a] Ulf Ellervik[a]*

[a] Center for Analysis and Synthesis, Center for Chemistry and Chemical Engineering, Lund University, P.O. Box 124, SE-221 00 Lund, Sweden

[b] Department of Experimental Medical Science, Lund University, BMC C12, SE-221 84 Lund, Sweden

[c] Department of Organic Chemistry, Arrhenius Laboratory, Stockholm University, SE-106 91 Stockholm, Sweden

[d] Institut de Chimie et Biochimie Moléculaires et Supramoléculaires (UMR 5246), Laboratoire de Chimie Organique 2, Université Claude Bernard Lyon 1 and CNRS; 43 Boulevard du 11 Novembre 1918, F-69622, Villeurbanne, France

Abstract

Xyloside analogs with substitution of the endocyclic oxygen atom for sulfur or carbon were investigated as substrates for β-1,4-galactosyltransferase 7 (β4GalT7), a key enzyme in the biosynthesis of GAG chains. The analogs with endocyclic sulfur proved to be excellent substrates for β4GalT7, and were galactosylated approximately 15 times more efficiently than the corresponding xyloside. The 5a-carba-β-xylopyranoside in the D-configuration proved to be a good substrate for β4GalT7 while the enantiomer in the L-configuration showed no activity. The pronounced activity of the sulfur analogs was further investigated by x-ray crystallography, NMR analysis, molecular modeling, and docking studies and showed a favorable interaction, i.e. a parallel displaced geometry, between the naphthyl moiety and a tyrosine side chain.

Introduction

β-1,4-galactosyltransferase 7, also known as β4GalT7 or GalT-I, is a key enzyme in the biosynthesis of glycosaminoglycan (GAG) chains. GAG chains are long linear polyanionic carbohydrates, often attached to a core protein to form a proteoglycan (PG). These

macromolecules are positioned in the extracellular matrix or on cell surfaces in mammalian cells and are involved in important biological processes such as proliferation, differentiation, adhesion, and migration. In addition, PGs and GAGs play important roles in cancer pathology, as well as in bacterial or viral infections.[1-4] The biosynthesis of PGs is initiated by the addition of xylose to a serine moiety of the core protein, followed by addition of two galactose units and a glucuronic acid unit, to form a linker tetrasaccharide that is the starting point for growing GAG chains. β4GalT7 catalyzes the addition of the first galactose unit to the xylose moiety, using UDP-α-D-galactose (UDP-Gal) as donor. In 1999, Almeida et al. cloned, expressed, and characterized β4GalT7 and identified it as a GalT-I enzyme.[5] In 2013, Qasba and co-workers published the crystal structures of two different conformations of human β4GalT7, one in the opened and one in the closed form, as well as the crystal structure of β4GalT7 from *Drosophila* with both acceptor and donor substrate present.[6] The crystal structures of human β4GalT7 reveal that conformational changes occur upon binding of UDP or UDP-Gal and Mn^{2+}, forming a hydrophobic, xylose-binding, acceptor pocket.

It has long been known that β-D-xylopyranosides bearing hydrophobic aglycon can enter cells and initiate the synthesis of GAG chains by acting as primers.[7-9] We have recently shown, using naphthyl xylosides as model compounds, that most modifications of the hydroxyl groups of the xylose unit rendered inactive compounds in terms of galactosylation by β4GalT7.[10] However, we and other groups have reported modifications of the xylose moiety, such as fluorination or epimerisation, that resulted in derivatives with inhibitory activity.[10-13] In contrast, modifications of the aglycon, the length of the spacer between the carbohydrate unit and the aromatic moiety, or the exocyclic atom, significantly influenced galactosylation by β4GalT7.[14] Thus, replacement of the anomeric oxygen with sulfur increased galactosylation, while the corresponding *C*-xyloside resulted in decreased activity (Figure 1).

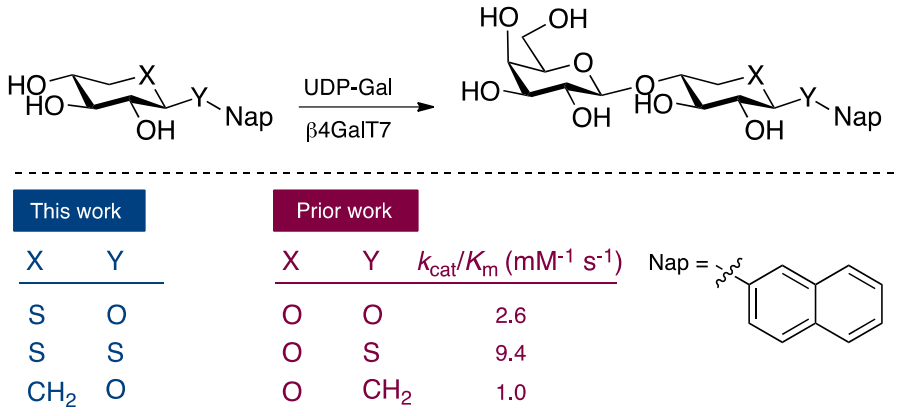

Figure 1. The effect of the endocyclic and exocyclic atom on β4GalT7 activity.

Interestingly, xyloside analogs where the endocyclic oxygen atom have been replaced by sulfur, e.g. Naroparcil, Beciparcil, Iliparcil, and Odiparcil, have been synthesized and investigated as antithrombotics (Figure 2).[15-18] The activity originates from their ability to form GAG chains that possess antithrombotic activity and it was shown that these compounds are indeed substrates for β4GalT7 and a trend in galactosylation was observed: β-D-xylosides < 1-thio-β-D-xylosides < 5-thio-β-D-xylosides < 1,5-dithio-β-D-xylosides.[15]

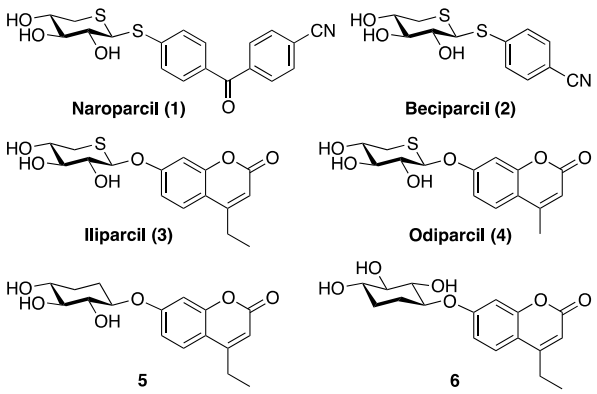

Figure 2. 5-Thio-β-D-xylopyranosides **1-4** and naphthyl 5a-carba-β-xylopyranosides **5** and **6**.

5a-Carba-xylosides have also been investigated as antithrombotic agents. The carbaxyloside analog of Iliparcil has been synthesized, as well as its L-xylo-enantiomer (Figure 2).[19-20] Remarkably, the authors propose that the L-xylo-derivative **6** shows much higher antithrombotic activity compared to the D-xylo-enantiomer **5** and that only the compound with L-xylo conformation functioned as substrate for β4GalT7 when assayed with enzyme extracts from chicken embryo. This is in stark contrast to other investigations where L-enantiomers of xylosides rarely exhibit any activity as a substrate for β4GalT7.[14, 20-22]

As part of our ongoing investigation to explore the active site of β4GalT7, we present the xyloside analogs naphthyl 5-thio- and naphthyl 1,5-dithio-β-D-xylopyranoside **9** and **10** as well as naphthyl 5a-carba-β-xylopyranoside **11** in both the D- and L-configuration (Figure 3). The compounds were studied in a β4GalT7 enzyme assay to determine their ability to act as substrates for β4GalT7 and to elucidate the role and function of the endocyclic oxygen atom as well as the role of the conformation of the carbaxylosides. Since the activity of previously published thio- and carba-analogs (Figure 2) has been tested with partially purified enzyme extracts from chicken embryos,[15-16, 20] we wanted to confirm the activity in a β4GalT7

assay using purified enzyme. In addition, we have studied xyloside **7** and 1,5-dithio-xyloside **10** by X-ray crystallography and performed NMR studies and molecular docking simulations to understand the difference in activity between the compounds. Our hypothesis is that the exchange of the endocyclic oxygen for sulfur, results in significant changes in the position of the aromatic moiety, which results in pronounced aromatic stacking between the naphthyl moiety in the xylosides with aromatic residues of the protein. These results open up for design of efficient GAG primers and inhibitors.

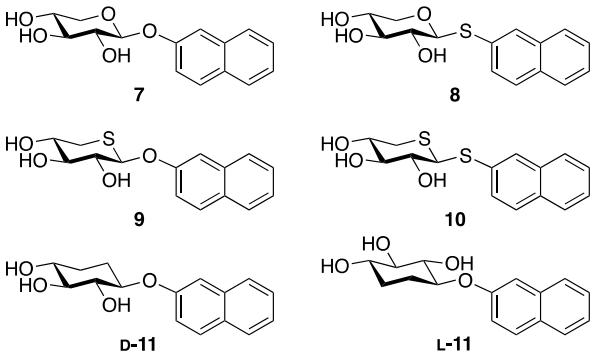

Figure 3. Structures of investigated xylosides and xyloside analogs.

Result and discussion

Synthesis

The thio derivatives **9** and **10** were synthesized from the known donor 2,3,4-tri-*O*-acetyl-5-thio-α-D-xylopyranosyl bromide **12** (Scheme 1).[23] The glycosylation reaction with 2-naphthol to form **13** turned out to be difficult, due to formation of the corresponding *C*-xyloside as the major product. Praly and coworkers reported that phenyl 2,3,4-tri-*O*-acetyl-5-thio-β-D-xylopyranoside is stable below -30 °C, but anomerization as well as rearrangement to the thermodynamically more stable *C*-xyloside occurs at 27 °C with catalytic amount of $BF_3{\cdot}Et_2O$.[24] In comparison, O→C rearrangement occurs much slower for the corresponding α-anomer, under similar conditions. Synthetic studies of the formation of Iliparcil (**3**) with different donors, promoters, solvents, and reaction conditions showed that the most effective glycosylation was obtained with the bromide donor and $ZnO\text{-}ZnCl_2$ as catalyst in toluene/acetonitrile at 60 °C.[25] By using this procedure, we isolated compound **13** in low yield as an α,β-mixture (0.9:1), together with C-xylosylated products. Reactions at other temperatures (-30 °C, rt, 60 °C) or in other solvents (CH_2Cl_2, toluene/DMF) did not improve the yield of the target compound, nor did reaction with $BF_3{\cdot}Et_2O$ or using phase transfer

conditions. Peracetylated 5-thio-D-xylopyranoside was also investigated as donor in presence of $BF_3{\cdot}Et_2O$. At -78 °C, with exclusive formation of the *C*-xyloside at -40 °C, 0 °C, and room temperature. The corresponding trichloroacetimidate donor was also tested, without success.

In contrast, the corresponding 1,5-dithio-xyloside **14** was formed in 54% yield from the donor **12** and 2-naphthalenethiol, using ZnO-$ZnCl_2$ as promoter. Deacetylation of **13** and **14** generated the target compounds **9** and **10**, where **9** had to be separated from the α-anomer by chromatography.

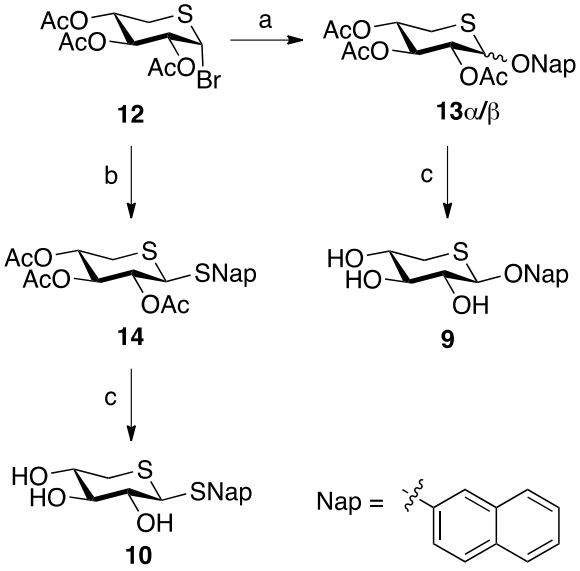

Scheme 1. Reagents and conditions: a) 2-naphthol, ZnO-ZnCl, toluene:MeCN (1:1), 13X sieves, 60 °C, 4 h, α/β 0.9:1; b) 2-naphthalenethiol, ZnO-ZnCl, toluene:MeCN (1:1), 13X sieves, 45 °C, 1.5 h, 54%; c) NaOMe (0.05 M), MeOH, **9**: 2% over two steps; **10**: 97%.

The syntheses of carba analogs **D-11** and **L-11** started from α,β-mixtures of the known D- and L-4,5,6-tris(benzyloxy)cyclohex-2-enol **15** (Scheme 2). The enol with D-xylo configuration **D-15** was synthesized according to published procedures from the commercially available methyl α-D-glucopyranoside.[26-27] The L-xylo analog **L-15** was instead obtained using similar synthetic methods according to published procedures via a route starting from D-xylose.[28-30] Mitsunobu reaction of the enols **D-15** and **L-15** generated **D-16** and **L-16** together with the corresponding α-anomers, Hydrogenation to remove the benzyl protective groups and to saturate the alkene moiety gave the 5a-carba-β-xylopyranosides **D-11** and **L-11**. The ability of the newly synthesized xyloside analogs **7-11** to act as substrates for β4GalT7 was then investigated in an enzymatic assay.

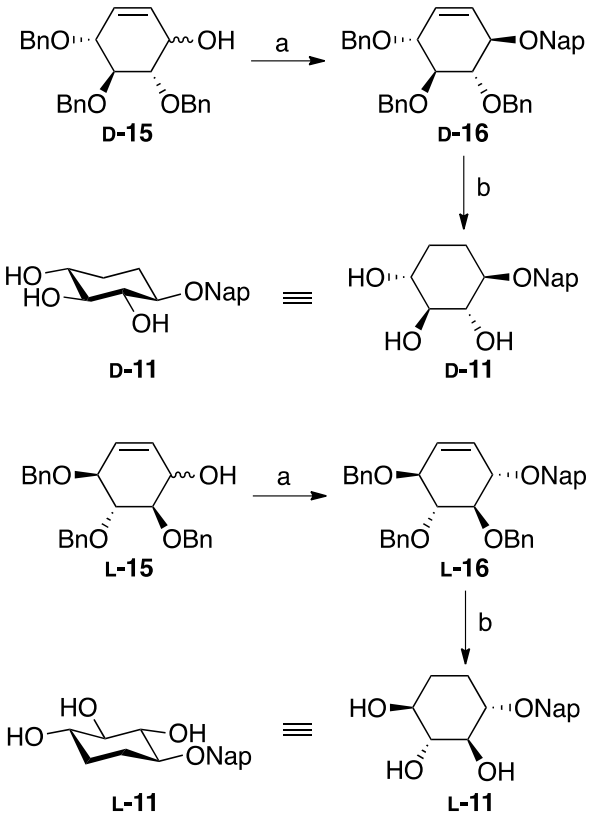

Scheme 2. Reagents and conditions: a) 2-naphthol, PPh_3, DIAD, THF, rt, 7h, 51% **D-16**, 24% **L-16**; b) H_2 (g), 10% Pd/C, HCl, DMF, rt, 5 h, **D-11**: 31%; **L-11**: 50%.

β4GalT7 assay

A slightly improved β4GalT7 assay was used,[10, 14] [ref till unpublished dideoxy paper] which is reflected in the kinetic parameters for the compounds analyzed (Table 1). For example, the K_m value for **7** was similar to previously reported values, whereas V_{max}, k_{cat} and k_{cat}/K_m differed significantly.

Table 1. Kinetic parameters for galactosylation of xyloside analogs **7-11** by β4GalT7.

Compound	K_m (μM)	V_{max} (pmol s^{-1})	k_{cat} (s^{-1})	k_{cat}/K_m (mM^{-1} s^{-1})
7	780	2.6	3.1	4.0
8	360	2.2	2.7	7.5
9	34	1.7	2.0	58.8
10	25	1.3	1.6	64.0
D-11	390	2.3	2.7	6.9

L-11	-	-	-	-

Compounds **7** and **8** have been investigated previously,[14] and were included as reference compounds due to the above-mentioned variations. Excess-substrate inhibition of the enzyme was observed for compounds **9** and **10** at 0.5 mM, and the kinetic parameters were calculated using the concentrations up to the highest observed reaction rate. The trend in galactosylation of the thio derivatives **8**-**10** by β4GalT7 was β-D-xyloside < 1-thio-β-D-xyloside < β4GalT7< 1,5-dithio-β-D-xyloside (Table 1). This is similar of what has been reported previously,[15] where the 5-thio-analog and 1,5-dithio-analog are excellent substrates for β4GalT7 and were galactosylated approximately 15 times more efficiently than the corresponding xylosides. Out of the two carbasugars, only **D-11** proved to be a substrate for β4GalT7 (Table 1). Interestingly, this is opposite of what has been reported previously.[19-20] The active compound **D-11** shows the same sign (-) of the specific rotation as the previously published active compound **6**. We thus propose that the carbasugars with D-configuration are the actual substrates for β4GalT7.

Earlier, we have observed that exchange of the exocyclic oxygen in compound **7** for sulfur, i.e. compound **8**, results in approximately 2-3 times better activity (k_{cat}/K_m) as substrate for β4GalT7, while the corresponding *C*-xyloside is less active by a factor of 2-3.[14] Interestingly, exchange of the endocyclic oxygen for carbon results slightly higher activity, while the corresponding sulfur analogs **8** and **9** are approximately 15 times better. From these data we propose that the ability of these compounds to act as substrates for β4GalT7 is dependent on both the endocyclic and the exocyclic oxygen atoms. While the exocyclic oxygen atom probably interacts with the protein, indicated by the reduced activity of the C-xyloside, it is reasonable to assume that modifications of the endocyclic oxygen atom results in conformational changes, that can be observed as pronounced activities as substrates for β4GalT7.

To elucidate why the 1,5-dithio-β-D-xyloside **10** is a such a good substrate for β4GalT7, compared to the β-D-xyloside **7**, we performed single-crystal X-ray diffraction studies of the two compounds.

Single-crystal X-ray diffraction studies

Crystals suitable for single-crystal X-ray diffraction of xyloside **7** could be obtained through slow crystallization in a methanol solution. The structure was found to crystallize in the orthorhombic space group $P2_12_12_1$ and displayed hydrogen bonds both between the adjacent

parent molecule as well as the co-crystallized methanol solvates. Similarly, the 1,5-dithio-xyloside **10** was crystallized from water, generating colorless needles. This structure crystallized in monoclinic $P2_1$, and featured hydrogen bonds to both other parent molecules and water solvates. The single-crystal X-ray structures, as well as an overlay of the structures of compounds **7** and **10** are shown in Figure 4. Important bond lengths and angles are summarized in Table 2. From the overlay structure we observe only minor differences in the position of the endocyclic oxygen and sulfur atoms. In contrast, the orientation and position of the aromatic naphthyl moiety is significantly shifted. In order to verify that the single-crystal X-ray structure of compound **10** is similar to the structure in solution, we performed an NMR-based conformational analysis.

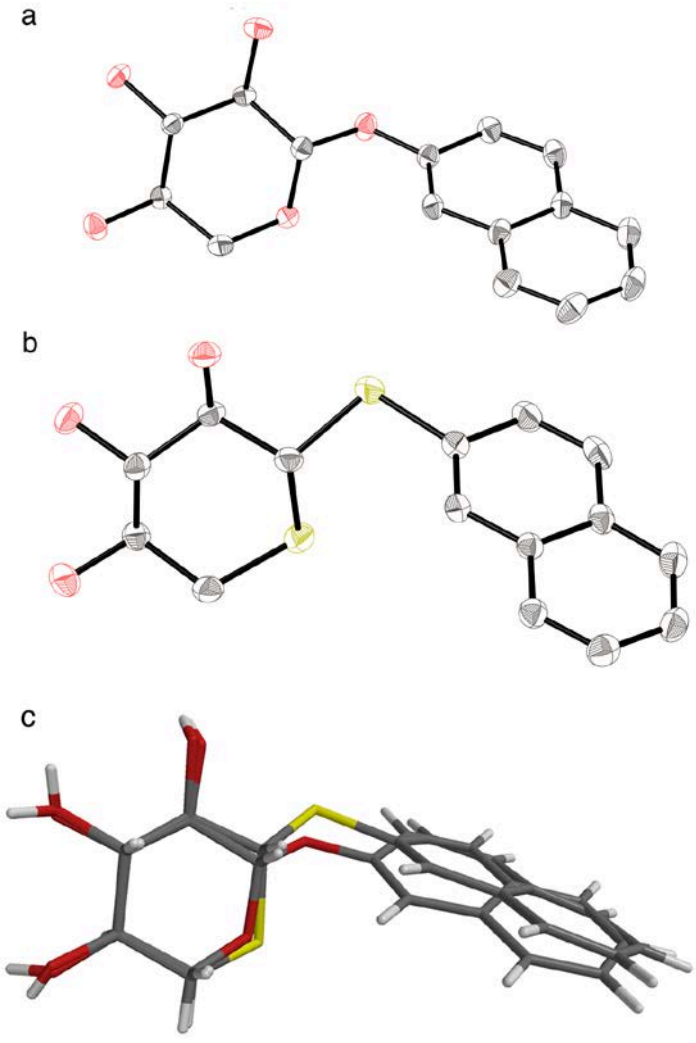

Figure 4. Thermal ellipsoid representations (atoms depicted at 30% probability level and hydrogen atoms excluded for clarity) of a) compound **7** and b) compound **10**. c) An overlay of

the single-crystal X-ray structures of **7** and **10**. Atoms C2, C3, C4 and C5 of the xyloside moiety were used as anchor points in the overlay structure.

Table 2. Bond lengths (Å) and angles from single-crystal X-ray structures of compounds **7** and **10**.

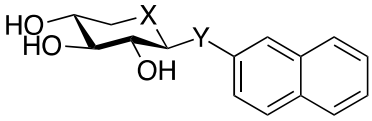

	7	**10**
C5-X	1.46	1.80
X-C1	1.42	1.81
C1-Y	1.41	1.81
X-C1-Y	107°	108°
C5-X-C1-Y	-175°	-175
X-Y	2.27	2.94
O3-O4	2.91	2.75
O2-O3	2.85	2.79

NMR-based conformational analysis

NMR parameters were determined for compound **10** at 37 °C. Some chemical shifts differed substantially compared to xyloside **7** due to the presence of two sulfur atoms in the molecule,[31] namely, H1, C1, H5 and C5, i.e., those adjacent to the ring sulfur atom. The experimentally determined $^{3}J_{HH}$ coupling constants for H1, H2 up to H4, $H5_{pro\text{-}S}$ were all large (~9-11 Hz) indicating that the $^{4}C_{1}$ chair is the major or exclusive conformation. Both the ^{1}H NMR chemical shifts and the $^{n}J_{HH}$ obtained by QM calculations are in good agreement with those from experiment. Furthermore, the $^{3}J_{HH}$ were also calculated for the QM and X-ray geometries of **10** employing the Karplus-type relationships developed by Altona and co-workers.[32] Again, the $^{3}J_{HH}$ values were in full agreement with experiment.

The 3D structure of **10** in solution was further investigated by measurement of $^{3}J_{CH}$ using a ^{1}H-detected 1DLR experiment where the heteronuclear couplings are observed in anti-phase and homonuclear couplings are present in-phase (Figure 5). Selective excitation at the resonance frequency of the C1 nucleus resulted in a large $^{3}J_{CH}$ coupling constant to $H5_{pro\text{-}S}$ and a small one to $H5_{pro\text{-}R}$ (Table 3), consistent with antiperiplanar and -synclinal arrangements in the $^{4}C_{1}$ conformation of **10**, respectively. Likewise, the $^{3}J_{C5,H1}$ is small in agreement with a □synclinal arrangement. Furthermore, $^{3}J_{C1,H2}$ was detectable, where the negative sign was inferred based on QM calculations. The magnitude of the exocyclic $^{3}J_{C2',H1}$ related to the ϕ torsion angle is indicative of a syn-conformation,[33] although the presence of a sulfur atom in the sugar ring will influence the parametrization of the Karplus-type relationship, like for

regular sugar residues with an oxygen atom in the ring.[34] Notably, the QM calculations of $^{n}J_{CH}$ using a geometry-optimized $^{4}C_{1}$ chair model, with the naphthyl group in a synclinal orientation (like in the X-ray structure), reproduced very well those observed experimentally (Table 3). Finally, with a plausible solution conformation of compound **10**, similar to the single crystal x-ray structure, we performed docking studies to determine the origin of the pronounced galactosylation of this compound by β4GalT7.

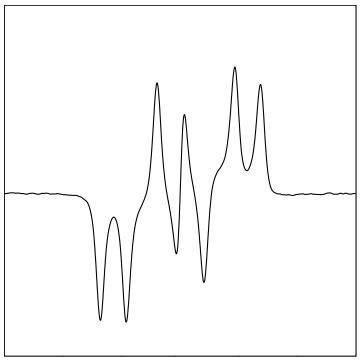

Figure 5. $^{13}C,^{1}H$-heteronuclear long-range spin-spin couplings observed in anti-phase using 1D ^{1}H-detected NMR experiments; homonuclear $J_{H,H}$ are observed in-phase. (a) C2',H1; (b) C5,H1; (c) C1,$H5_{pro\text{-}S}$.

Table 3. NMR parameters for compound **10**.

	1	2	3	4	5

Expt	^{1}H	4.103	3.446	3.202	3.612	2.668, 2.573
	$^{n}J_{HH}$	10.19	8.69	9.02	10.93, 4.34	–13.45[a]
	^{13}C	54.99	77.23	80.59	74.43	34.82
QM	^{1}H	3.919	3.396	3.182	3.811	2.845, 2.633
	$^{n}J_{HH}$	10.88	8.74	8.93	11.14, 5.26	–14.65
MSpin (QM)	$^{3}J_{HH}$	10.60	9.43	9.36	11.45, 4.18	n.d.
MSpin (Crystal)	$^{3}J_{HH}$	11.02	9.46	9.37	11.59, 3.39	n.d.
		C1-H2	C1-H5$_{pro-R}$	C1-H5$_{pro-S}$	C5-H1	C2'-H1
Expt	$^{n}J_{CH}$	–1.67[a]	2.18	9.25	1.54	4.11
QM	$^{n}J_{CH}$	–1.58	1.22	10.30	0.67	5.14

^{1}H and ^{13}C NMR chemical shifts are given in ppm and spin-spin coupling constants in Hertz. For the methylene group, the pro-*R* proton is given prior to the pro-*S* proton. Entries for MSpin are based on either QM geometry optimizations or from the crystal structure. [a] Sign assumed negative based on QM calculation.

Molecular Docking Simulations

The resulting poses from the docking simulations were categorized in two groups, viz., those with the xylose moiety oriented in the binding site in a similar fashion to those previously reported with the aglycon stacked parallel to Y179 and the xylose moiety oriented above Y177,[14] and non-productive ones with the aglycon in the binding site close to UDP-Gal. In the cases where the naphthyl group was stacked above Y179, the top-ranked poses were essentially identical, both structures showing a parallel displaced geometry[35] with an angle of 8.95° between the planes and the center of gravity for the two ring systems separated by 3.83 Å. The displacement of the naphthyl center was 0.79 Å from the middle of the tyrosine ring (Figure 6). It has been shown that either a parallel displacement or a T-shaped stacking is preferred for naphthyl-benzene systems;[36] the orientation of the aglycon is in good agreement with a parallel displaced geometry. It is reasonable to assume that the pronounced galactosylation of compound **10** by β4GalT7 can be explained by this favorable aromatic stacking, induced by the exchange of both the exocyclic and the endocyclic oxygen atoms for sulfur.

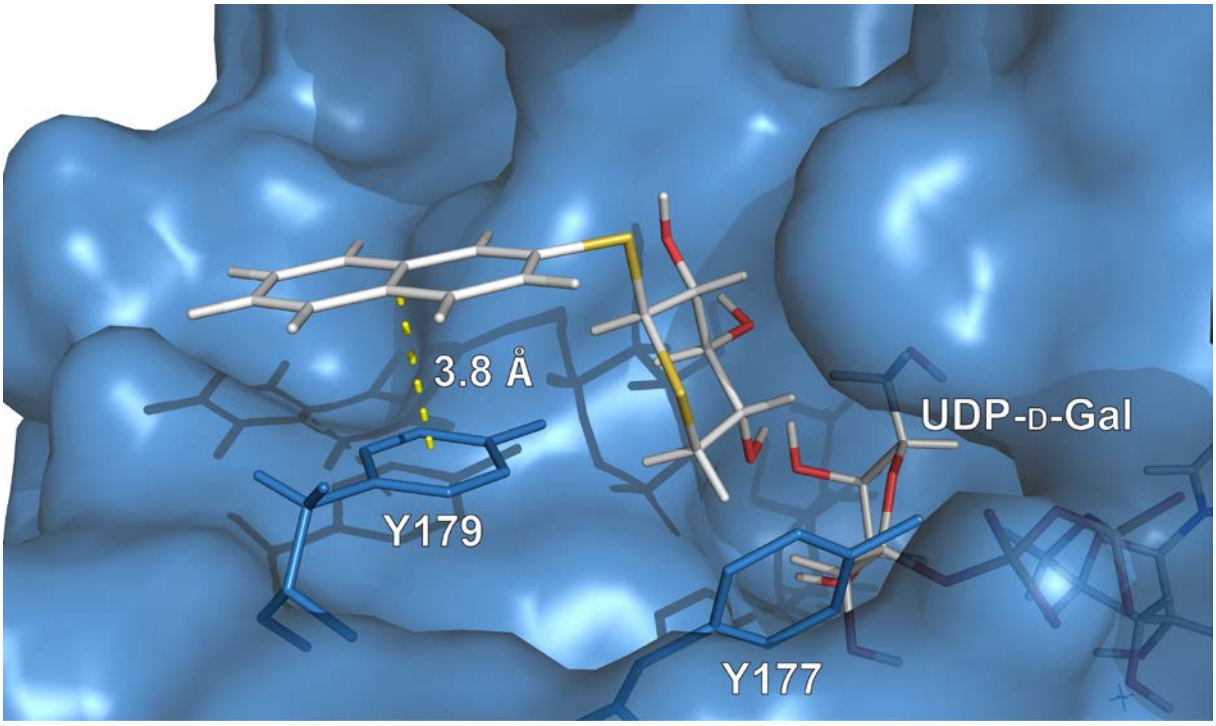

Figure 6. Molecular docking complex of compound **10** and β4GalT7 mutant D211N (Drosophgila) for the top-ranked pose with the xylose moiety oriented in the active site. The naphthyl group of the ligand is positioned above Y179 such that a parallel displaced geometry is obtained.

Conclusions

We have synthesized a series of xyloside analogs with substitution of the endocyclic oxygen for sulfur or carbon. The analogs with endocyclic sulfur proved to be excellent substrates for β4GalT7 and galactosylation occurred approximately 15 times more efficiently than with the corresponding xylosides. Furthermore we have shown that the 5a-carba-β-xylopyranoside in the D-configuration is a good substrate for β4GalT7 while the enantiomer in the L-configuration showed no activity. Molecular modeling, and X-ray crystallography indicate that the exchange of the endocyclic oxygen for sulfur give rise to conformational changes and a favorable aromatic stacking of the naphthyl moiety with tyrosine 179 of the protein.

Experimental procedures

Synthesis

General

All solvents were dried using MBRAUN SPS-800 Solvent purification system prior to use, unless otherwise stated. The purchased reagents were used without further purification.

Reactions were monitored by TLC using alumina plates coated with silica gel, and visualized using UV light or by charring with an ethanolic anisaldehyde solution. Biotage Isolute phase separators were used for drying of combined organic layers. Preparative chromatography was performed on Biotage Isolera One flash purification system using Biotage SNAP KP-Sil silica cartridges. Agilent Technologies 1260 Infinity HPLC with Waters Symmetry C18 column, 5 μm, 19 × 100 mm, gradient of MeCN in H_2O (0.1% formic acid) was used for purification. Optical rotations were measured on Perkin Elmer instruments, Model 341 polarimeter and are reported as $[\alpha]_D^T$ (*c* = g/100 mL), D indicate the sodium D line (589 nm) and T indicates the temperature. NMR spectra were recorded on Bruker Avance II at 400 MHz (^{1}H) and 100 MHz (^{13}C) and assigned using 2D methods (COSY, HMQC). Chemical shifts are reported in ppm downfield from Me_4Si, with reference to residual solvent peaks (δH $CDCl_3$ = 7.26 ppm, MeOH-d_4 = 3.31 ppm, $(CD_3)_2CO$ = 2.05 ppm) and solvent signals (δC $CDCl_3$ = 77.0 ppm, MeOH-d_4 = 49.0 ppm, $(CD_3)_2CO$ = 29.84). Mass spectra were recorded on Waters XEVO G2 (Positive ESI).

Synthesis and physical characterization of 2,3,4-tri-O-acetyl-5-thio-α-D-xylopyranosyl bromide **12**[23] and 4,5,6-tris(benzyloxy)cyclohex-2-enol **D-15**[26-27] and **L-15**[28-30] have been described before. For **D-15** and **L-15** the method developed for affecting the diastereomeric outcome of the Grignard reaction was utilized where $MgBr_2{\cdot}EtO_2$ was added and the solvent of the commercial vinylmagnesium bromide was changed from THF to CH_2Cl_2.[30] The analyses of the products were in accordance with published data. 2-Naphthyl β-D-xylopyranoside **7** was crystallized from MeOH as colorless needles.

2-Naphthyl 5-thio-β-D-xylopyranoside (9)

ZnO (120 mg, 1.48 mmol) and $ZnCl_2$ (201 mg, 1.48 mmol) were added to a stirred solution of 2-naphthol (213 mg, 1.48 mmol) in toluene:MeCN (1:1, 20 mL) containing 13X molecular sieves. The mixture was heated to 60°C, and after 20 min, **12** (500 mg, 1.41 mmol) was added. Heating was removed after 4h, upon the reaction mixture was diluted with CH_2Cl_2 and filtered through Celite®. The filtrate was washed with satd aq $NaHCO_3$ and brine, dried, and concentrated. Column chromatography (petroleum ether:EtOAc 8:2 → 2:1) gave **13** (48 mg) as a anomeric mixture (α:β 0.9:1) as well as a mixture of *C*-xylosylated products (60 mg) as a anomeric mixture (α:β 0.2:1). The crude mixture of **13** (48 mg) was used without further purification, and dissolved in MeOH (9.5 mL), to which NaOMe (1M in MeOH, 0.5 mL) was

added. After 3 h, the reaction was neutralized with acetic acid and concentrated. HPLC gave **9** (8 mg, 2%) as a white solid. $[\alpha]_D^{20}$ -88 (*c* 0.4, MeOH); ^{1}H-NMR (CD_3OD) δ 7.79-7.78 (m, 3H, ArH), 7.55 (d, 1H, *J* = 2.5 Hz, ArH), 7.46-7.42 (m, 1H, ArH), 7.37-7.33 (m, 1H, ArH), 7.27 (dd, 1H, *J* = 2.5, 9.0 Hz, ArH), 5.25 (d, 1H, *J* = 8.7 Hz, H-1), 3.84 (t, 1H, *J* = 8.8 Hz, H-2), 3.72 (td, 1H, *J* = 5.5, 9.2 Hz, H-4), 3.32 (t, 1H, *J* = 9.0 Hz, H-3), 2.78-2.68 (m, 2H, H-5ax, H-5eq); ^{13}C-NMR (CD_3OD) δ 156.7, 135.8, 131.1, 130.3, 128.6, 128.1, 127.4, 125.2, 120.0, 111.2, 82.7, 78.5, 78.3, 74.4, 31.1; HRMS (ESI): *m/z* $[M + Na]^+$ calcd for $C_{15}H_{16}O_4SNa$: 315.0668; found: 315.0667.

2-Naphthyl 1,5-dithio-β-D-xylopyranoside (10)

Compound **14** (100 mg, 0.230 mmol) was dissolved in MeOH (28.5 mL) and NaOMe (1M in MeOH, 1.5 mL) was added. After 1h, the reaction was neutralized with acetic acid and concentrated. Column chromatography (CH_2Cl_2:MeOH 98:2 $\rightarrow$ 88:12) gave **10** (69 mg, 97%) as a white solid that crystallized from H_2O as colorless needles. $[\alpha]_D^{20}$ +41 (*c* 0.7, $CHCl_3$); ^{1}H-NMR (CD_3OD) δ 8.07 (d, 1H, *J* = 1.4 Hz, ArH), 7.85-7.80 (m, 3H, ArH), 7.63 (dd, 1H, *J* = 1.9, 8.6 Hz, ArH), 7.52-7.46 (m, 2H, ArH), 4.10 (d, 1H, *J* = 10.2 Hz, H-1), 3.59 (ddd, 1H, *J* = 4.5, 9.1, 10.8 Hz, H-4), 3.42 (dd, 1H, *J* = 8.7, 10.2 Hz, H-2), 3.18 (t, 1H, *J* = 8.9 Hz, H-3), 2.66 (dd, 1H, *J* = 10.8, 13.4 Hz, H-5ax), 2.55 (dd, 1H, *J* = 4.6, 13.4 Hz, H-5eq); ^{13}C-NMR (CD_3OD) δ 135.0, 134.1, 132.7, 131.7, 121.0, 129.3, 128.7, 128.6, 127.6, 127.5, 80.5, 77.2, 74.4, 54.9, 34.8; HRMS (ESI): *m/z* $[M + Na]^+$ calcd for $C_{15}H_{16}O_3S_2Na$: 331.0437; found: 331.0439.

(1*R*,2*S*,3*R*,4*R*)-4-(2-Naphthyloxy)cyclohexan-1,2,3-triol (D-11)

H_2 (g) was applied to a stirred mixture of 10% Pd/C (20 mg), conc HCl (0.02 mL, 2.4 mmol), and dry DMF (1 mL) at rt and under atmospheric pressure and after 10 minutes, **D-16** (58 mg, 0.11 mmol) in dry DMF (1 mL) was added and more H_2 (g) was applied. After 20 h, Et_3N was added until neutral pH and the reaction mixture was filtered through celite, eluted with CH_2Cl_2 (5 mL). H_2O (10 mL) was added and the aqueous phase was extracted with CH_2Cl_2 (3x 5 mL). The combined organic phases were washed with brine and dried before concentrated. Column chromatography (SiO_2, CH_2Cl_2:MeOH 95:5) gave **D-11** (9 mg, 31%) as a white solid. $[\alpha]_D^{20}$ -27 (*c* 0.8, CD_3OD); ^{1}H-NMR ($(CD_3)_2CO$) δ 7.80-7.75 (m, 3H), 7.44-7.40 (m, 2H), 7.33-7.29 (m, 1H), 7.18 (dd, 1H, *J* = 2.6, 9.0 Hz), 4.40-4.33 (m, 1H), 3.55 (t, 1H, *J* = 9.2 Hz), 3.52-3.47 (m, 1H), 3.30 (t, 1H, *J* = 9.0 Hz), 2.24-2.19 (m, 1H), 1.94-1.89 (m, 1H), 1.55-1.38 (m, 2H); ^{13}C-NMR ($(CD_3)_2CO$) δ 157.5, 135.7, 130.03, 129.96, 128.4, 127.6, 127.0, 124.3, 120.6, 109.6,

80.2, 79.2, 77.0, 73.0, 29.1, 26.5; HRMS (ESI): *m/z* $[M + Na]^+$ calcd for $C_{16}H_{18}O_4Na$: 297.1103; found: 297.1104.

(1*S*,2*R*,3*S*,4*S*) 4-(2-Naphthyloxy)cyclohexan-1,2,3-triol (L-11)

H_2 (g) was applied to a stirred mixture of 10% Pd/C (32 mg), conc HCl (55 µL, 0.66 mmol), and DMF (2.5 mL) at rt. **L-16** (17 mg, 0.030 mmol) in DMF (2.5 mL) was added to the mixture, purged with H_2-gas twice and left under H_2. After 20h, Et_3N was added until neutral pH and the reaction mixture was filtered and concentrated. Column chromatography (CH_2Cl_2:MeOH 97:3 → 91:9) and HPLC gave **L-11** (20 mg, 50%) as a white solid. $[\alpha]_D^{20}$ +23 (*c* 0.7, CD_3OD); ^{1}H-NMR ($(CD_3)_2CO$) δ7.80-7.75 (m, 3H), 7.44-7.40 (m, 2H), 7.33-7.29 (m, 1H), 7.18 (dd, 1H, *J* = 2.6, 9.0 Hz), 4.39-4.33 (m, 1H), 3.55 (t, 1H, *J* = 9.2 Hz), 3.52-3.47 (m, 1H), 3.30 (t, 1H, *J* = 9.0 HZ), 2.23-2.19 (m, 1H), 1.94-1.89 (m, 1H), 1.55-1.38 (m, 2H); ^{13}C-NMR ($(CD_3)_2CO$) δ 157.5, 135.7, 130.0, 129.9, 128.3, 127.6, 127.0, 124.3, 120.5, 109.6, 80.2, 79.2, 77.0, 73.0, 29.1, 26.5; HRMS (ESI): *m/z* $[M + Na]^+$ calcd for $C_{16}H_{18}O_4Na$: 297.1103; found: 297.1103.

2-Naphthyl 2,3,4-tri-*O*-acetyl-1,5-dithio-β-D-xylopyranoside (14)

ZnO (101 mg, 1.24 mmol) and $ZnCl_2$ (169 mg, 1.24 mmol) were added to a stirred solution of 2-naphthalenethiol (199 mg, 1.24 mmol) in toluene:MeCN (1:1, 10 mL) containing 13X molecular. The mixture was heated to 45 °C, and after 20 min, **12** (400 mg, 1.126 mmol) was added. Heating was removed after 1h, upon the reaction mixture was diluted with CH_2Cl_2 and filtered through Celite®. The filtrate was washed with satd aq $NaHCO_3$ and brine, dried, and concentrated. Column chromatography (pet ether:EtOAc 90:10 → 77:23) gave **14** (265 mg, 54%) as a white solid. $[\alpha]_D^{20}$ +25 (*c* 0.6, MeOH); ^{1}H-NMR ($CDCl_3$) δ8.03 (d, 1H, *J* = 1.7 Hz, ArH), 7.85-7.81 (m, 3H, ArH), 7.57 (dd, 1H, *J* = 1.9, 8.6 Hz, ArH), 7.53-7.51 (m, 2H, ArH), 5.23 (dd, 1H, *J* = 9.2, 10.4 Hz, H-2), 5.10-5.01 (m, 2H, H-3, H-4), 4.14 (d, 1H, *J* = 10.6 Hz, H-1), 2.80 (dd, 1H, *J* = 4.2, 13.5 Hz, H-5eq), 2.67 (dd, 1H, *J* = 10.5, 13.5 Hz, H-5ax), 2.10 (s, 3H, OAc), 2.03 (s, 3H, OAc), 2.00 (s, 3H, OAc); ^{13}C-NMR ($CDCl_3$) δ 169.9, 169.8, 169.7, 133.6, 133.4, 133.1, 130.4, 128.94, 128.87, 127.90, 127.88, 127.1, 126.9, 74.2, 74.1, 72.4, 52.3, 31.5, 20.9, 20.8, 20.7; HRMS (ESI): *m/z* $[M + NH_4]^+$ calcd for $C_{21}H_{26}NO_6S_2$: 452.1202; found: 452.1198.

(3*R*,4*S*,5*S*,6*R*)-3,4,5-Trisbenzyloxy-6-(2-naphthyloxy)-cyclohex-1-en (D-16) and (3*R*,4*S*,5*S*,6*S*)-3,4,5-trisbenzyloxy-6-(2-naphthyloxy)cyclohex-1-en

DIAD (68 μL, 0.32 mmol) was added to a stirred solution of 2-naphthol (37 mg, 0.27 mmol), PPh_3 (85 mg, 0.32 mmol), and **D-15**[27] (1*S*:1*R* 5:1) (90 mg, 0.22 mmol) in THF (2 mL). After 7 h, the reaction mixture was concentrated and the crude residue was purified by column chromatography (Heptane:EtOAc 100:0→92:8) to give (3*R*,4*S*,5*S*,6*S*)-3,4,5-trisbenzyloxy-6-(2-naphthyloxy)cyclohex-1-en (13 mg, 11%) and **D-16** (58 mg, 51%) as white amorphous solids. **D-16**: $[\alpha]_D^{20}$ -61 (*c* 1, $CHCl_3$); ^{1}H-NMR ($CDCl_3$) δ 7.78 (d, 1H, *J* = 8.4 Hz), 7.77 (d, 1H, *J* = 8.8 Hz), 7.70 (d, 1H, *J* = 8.0 Hz), 7.46-7.42 (m, 1H), 7.38-7.28 (m, 11H), 7.22-7.15 (m, 7H), 5.84 (s, 2H), 5.16 (dd, 1H, *J* = 2.4, 7.2 Hz), 4.99 (d, 1H, *J* = 10.8 Hz), 4.89 (d, 1H, *J* = 10.8 Hz), 4.88 (d, 1H, *J* = 10.8 Hz), 4.84 (d, 1H, *J* = 10.8 Hz), 4.77 (d, 1H, *J* = 11.6 Hz), 4.73 (d, 1H, *J* = 11.6 Hz), 4.31 (dd, 1H, *J* = 3.2, 7.6 Hz), 3.96 (dd, 1H, *J* = 7.3, 10.2 Hz), 3.88 (dd, 1H, *J* = 7.6, 10.4 Hz); ^{13}C-NMR ($CDCl_3$) δ 155.9, 138.8, 138.5, 138.4, 134.6, 129.8, 129.4, 129.1, 128.6, 128.5, 128.38, 128.37, 128.2, 128.0, 127.9, 127.8, 127.7, 127.0, 126.6, 126.3, 124.0, 119.5, 109.0, 83.6, 83.1, 80.1, 79.2, 75.83, 75.76, 72.8; HRMS (ESI): *m/z* $[M + Na]^+$ calcd for $C_{37}H_{34}O_4Na$: 565.2355; found: 565. 2357. (3*R*,4*S*,5*S*,6*S*)-3,4,5-Trisbenzyloxy-6-(2-naphthyloxy)cyclohex-1-en: $[\alpha]_D^{20}$ +66 (*c* 0.7, $CHCl_3$); ^{1}H-NMR ($CDCl_3$) δ 7.79-7.74 (m, 2H), 7.69 (d, 1H, *J* = 8.0 Hz), 7.46-7.29 (m, 13H), 7.25-7.21 (m, 6H), 6.04 (ddd, 1H, *J* = 2.0, 4.8, 10.0 Hz), 5.93 (dd, 1H, *J* = 2.4, 10.4 Hz), 5.04-5.01 (m, 2H), 4.89 (d, 1H, *J* = 10.8 Hz), 4.80-4.69 (m, 4H), 4.32 (dd, 1H, *J* = 7.2 Hz, 10.0 Hz), 4.16 (dt, 1H, *J* = 2.0, 7.2 Hz), 3.76 (dd, 1H, *J* = 3.8 Hz, 9.8Hz); ^{13}C-NMR ($CDCl_3$) δ 156.4, 139.0, 138.6, 138.4, 134.5, 132.2, 129.6, 129.4, 128.6, 128.5, 128.4, 128.2, 128.1, 128.0, 127.82, 127.79, 127.76, 127.7, 126.9, 126.4, 124.9, 123.9, 120.2, 109.5, 79.9, 79.8, 78.6, 75.2, 73.0, 72.3, 72.1; HRMS (ESI): *m/z* $[M + Na]^+$ calcd for $C_{37}H_{34}O_4Na$: 565.2355; found: 565.2356.

(3*S*,4*R*,5*R*,6*S*) 3,4,5-Trisbenzyloxy-6-(2-naphthyloxy)-cyclohex-1-en (L-16)

PPh_3 (361 mg, 1.38 mmol), 2-naphthol (172 mg, 1.20 mmol), and DIAD (271 μL, 1.38 mmol) were added to a solution of **L-15**[29-30] (1*S*:1*R* 1:5) (382 mg, 0.917 mmol) in THF (46 mL). After 2h, the reaction mixture was concentrated and the crude residue was purified by column chromatography (heptane:EtOAc 99:1 → 85:15) to give **L-16** (121 mg, 24%) as a clear oil. $[\alpha]_D^{20}$ +63 (*c* 0.9, $CHCl_3$); ^{1}H-NMR ($CDCl_3$) δ 7.78 (d, 1H, *J* = 7.6 Hz), 7.77 (d, 1H, *J* = 8.9 Hz), 7.70 (d, 1H, *J* = 8.2 Hz), 7.46-7.42 (m, 1H), 7.39-7.28 (m, 11H), 7.22-7.15 (m, 7H), 5.84 (s, 2H), 5.16 (dd, 1H, *J* = 2.8, 7.4 Hz), 4.99 (d, 1H, *J* = 10.9 Hz), 4.89 (d, 1H, *J* = 10.9 Hz), 4.88 (d, 1H, *J* = 10.8 Hz), 4.84 (d, 1H, *J* = 10.8 Hz), 4.77 (d, 1H, *J* = 11.6 Hz), 4.72 (d, 1H, *J* = 11.6 Hz), 4.31 (dd, 1H, *J* = 2.8, 7.5 Hz), 3.95 (dd, 1H, *J* = 7.5, 10.5 Hz), 3.88 (dd, 1H, *J* = 7.5,

10.5 Hz); ^{13}C-NMR ($CDCl_3$) δ 155.9, 138.8, 138.43, 138.36, 134.6, 129.8, 129.3, 129.1, 128.6, 128.5, 128.36, 128.35, 128.1, 128.0, 127.9, 127.8, 127.7, 127.0, 126.6, 126.2, 124.0, 119.5, 109.0, 83.6, 83.1, 80.1, 79.2, 75.8, 75.7, 72.8; HRMS (ESI): *m/z* $[M + NH_4]^+$ calcd for $C_{37}H_{38}NO_4$: 560.2799; found: 560.2801.

β4GalT7 assay

Human β4GALT7 was expressed as a 6xHIS+GST fusion protein as previously reported, but slight changes were made in the purification protocol.[10, 14] Briefly, instead of a HisTrap HP (GE Life Sciences) column and manual purification, a HisTrap FF crude (GE Life Sciences) column and an ÄKTA start (GE Life Sciences) chromatography system was used during purification. β4GalT7 activity was determined essentially as previously described, but in a 96-well format.[10, 14] Briefly, in a 96-well polypropylene plate 50 ng of β4GalT7 was mixed with 1 mM UDP-Gal and various concentrations of xyloside analogs, in a total volume of 50 µL MES buffer (20 mM, pH 6.2) supplemented with $MnCl_2$ (10 mM). The plate was covered with a PES/silicone sealing film and incubated at 37 °C for 30 min in an Eppendorf Thermomixer C, with shaking at 800 rpm. After incubation, the plate was quickly transferred to a 4 °C cooling block and 1 µl from each well was transferred to a new 96-well polypropylene plate containing 100 µl HPLC eluent (70% NH_4OAc (60 mM, pH 5.6) - 30% CH_3CN (v/v)) in each well. The plate was mixed manually and centrifuged briefly before HPLC analysis as previously described. The results were plotted in GraphPad Prism 7.0a, using the nonlinear regression to the Michaelis-Menten model.

Single-Crystal X-ray Diffraction

Single crystals were used for full data collection on automatic diffractometers at room temperature. Data were measured on an Oxford Diffraction Xcalibur diffractometer with a Mo-Kα (λ = 0.71069 Å) from an enhanced optic X-ray tube operating at 50 kV and 40 mA, and a CCD plane detector. Run list generation and processing of the frame data and numerical absorption corrections were carried out using the Crysalis software package.[37] The charge flipping method as implemented in Superflip[38], was used for structure solution. The images were rendered using the program Crystalmaker, version 9.2c.[39]

NMR spectroscopy

NMR experiments for ^{1}H and ^{13}C NMR chemical shift assignments of compound **10** at 37 °C as well as ^{1}H NMR spin simulations were performed as previously described.[31] The one-

dimensional long-range (1DLR) experiment devised by Nishida et al.[40-41] was used to measure the $^{3}J_{CH}$ coupling constants for compound **10** (3.5 mg in 0.55 mL of methanol-d_4) by a ^{13}C site-selective excitation using Gaussian shaped pulses of 80 ms duration on a Bruker AVANCE III 700 MHz spectrometer equipped with 5 mm TCI Z-Gradient CryoProbe. The delay used for suppression of $^{1}J_{CH}$ was set to (145 Hz)$^{-1}$ and the time of the delay between excitation and coherence transfer, for evolution of the long-range coupling, was set to 83 ms. A spectral width of 12 ppm was sampled with 34 962 data points using 20k transients and an acquisition time of 2.1 s. Zero-filling was performed to 131k data points and an exponential line-broadening function lb = 0.6 Hz was used. Subsequently, the $^{3}J_{CH}$ coupling constants were extracted by the *J* doubling methodology[42] implemented in-house by a MATLAB script. ^{1}H chemical shifts and $^{n}J_{HH}$ coupling constants were determined with an iterative total-line shape analysis employing spin-spin simulation with the program PERCH[43]. $^{3}J_{HH}$ coupling constants for compound **10** were calculated using MSpin 1.3.3-79[44] and the JCoupling module, with the Altona parameter set[32] based on geometries retrieved from either QM geometry optimizations or crystal structures.

Quantum Mechanical Calculations

NMR parameters of compound **10** were calculated using the Gaussian09RevD.01 program suite[45]. Structures were first optimized using the B3LYP functional[46-47] and a 6-31G(d,p) basis set in gas phase and subsequently isotropic shielding constants, $^{3}J_{CH}$ and $^{3}J_{HH}$ values were calculated using the Gauge-Independent Atomic Orbital method (GIAO)[48-49] and DFT using the B3LYP functional, a 6-311+G(d,p) basis set; solvent effects were considered with a conductor-like polarizable continuum model (CPCM)[50-51] where methanol was given as the solvent. The keyword *mixed* was used to force a two-step calculation process, in the first step the Fermi contact contribution is calculated by uncontracting the basis set and adding a tight polarization function to the core, and in the second step the remaining three terms are calculated with the basis set as given[52]. Chemical shifts were then calculated from the isotropic shielding constants using empirical scaling according to the CHEmical SHIft REpository[53]. The slope was set to −1.095 and the intercept to 31.9072, in accordance with the previously specified level of theory and solvent.

Docking Simulations

Molecular docking was carried out as previously described.[14] The geometry obtained from the quantum mechanical calculations described above was used for the ligand input.

Acknowledgements

This work was supported by grants from the Crafoord Foundation, Lars Hiertas Memorial Foundation, the Magnus Bergvall Foundation, the Medical Faculty of Lund University, Lund University, the Royal Physiographic Society in Lund, the Swedish Research Council (No. 621-2013-4859), and The Knut and Alice Wallenberg Foundation.

References

1. Kamhi, E.; Joo Eun, J.; Dordick Jonathan, S.; Linhardt Robert, J. *Biol. Rev.* **2013**, *88*, 928-943.
2. Afratis, N.; Gialeli, C.; Nikitovic, D.; Tsegenidis, T.; Karousou, E.; Theocharis, A. D.; Pavao, M. S.; Tzanakakis, G. N.; Karamanos, N. K. *Febs J.* **2012**, *279*, 1177-1197.
3. Yamada, S.; Sugahara, K. *Curr. Drug Discovery Technol.* **2008**, *5*, 289-301.
4. Yip, G. W.; Smollich, M.; Götte, M. *Mol. Cancer Ther.* **2006**, *5*, 2139-2148.
5. Almeida, R.; Levery, S. B.; Mandel, U.; Kresse, H.; Schwientek, T.; Bennett, E. P.; Clausen, H. *J. Biol. Chem.* **1999**, *274*, 26165-26171.
6. Tsutsui, Y.; Ramakrishnan, B.; Qasba, P. K. *J. Biol. Chem.* **2013**, *288*, 31963-31970.
7. Okayama, M.; Kimata, K.; Suzuki, S. *J. Biochem.* **1973**, *74*, 1069-1073.
8. Schwartz, N. B.; Galligani, L.; Ho, P.-L.; Dorfman, A. *Proc. Natl. Acad. Sci. U. S. A.* **1974**, *71*, 4047-4051.
9. Robinson, H. C.; Brett, M. J.; Tralaggan, P. J.; Lowther, D. A.; Okayama, M. *Biochem. J.* **1975**, *148*, 25-34.
10. Siegbahn, A.; Manner, S.; Persson, A.; Tykesson, E.; Holmqvist, K.; Ochocinska, A.; Roennols, J.; Sundin, A.; Mani, K.; Westergren-Thorsson, G.; Widmalm, G.; Ellervik, U. *Chem. Sci.* **2014**, *5*, 3501-3508.
11. Saliba, M.; Ramalanjaona, N.; Gulberti, S.; Bertin-Jung, I.; Thomas, A.; Dahbi, S.; Lopin-Bon, C.; Jacquinet, J.-C.; Breton, C.; Ouzzine, M.; Fournel-Gigleux, S. *J. Biol. Chem.* **2015**, *290*, 7658-7670.
12. Tsuzuki, Y.; Nguyen, T. K. N.; Garud, D. R.; Kuberan, B.; Koketsu, M. *Bioorg. Med. Chem. Lett.* **2010**, *20*, 7269-7273.
13. Garud, D. R.; Tran, V. M.; Victor, X. V.; Koketsu, M.; Kuberan, B. *J. Biol. Chem.* **2008**, *283*, 28881-28887.
14. Siegbahn, A.; Thorsheim, K.; Staahle, J.; Manner, S.; Hamark, C.; Persson, A.; Tykesson, E.; Mani, K.; Westergren-Thorsson, G.; Widmalm, G.; Ellervik, U. *Org. Biomol. Chem.* **2015**, *13*, 3351-3362.
15. Bellamy, F.; Barberousse, V.; Martin, N.; Masson, P.; Millet, J.; Samreth, S.; Sepulchre, C.; Theveniaux, J.; Horton, D. *Eur. J. Med. Chem.* **1995**, *30*, 101s-115s.
16. Masson, P. J.; Coup, D.; Millet, J.; Brown, N. L. *J. Biol. Chem.* **1995**, *270*, 2662-2668.
17. Toomey, J. R.; Abboud, M. A.; Valocik, R. E.; Koster, P. F.; Burns-Kurtis, C. L.; Pillarisetti, K.; Danoff, T. M.; Erhardt, J. A. *J. Thromb. Haemost.* **2006**, *4*, 1989-1996.
18. Myers, A. L.; Upreti, V. V.; Khurana, M.; Eddington, N. D. *J. Clin. Pharmacol.* **2008**, *48*, 1158-1170.
19. Jeanneret, V.; Vogel, P.; Renaut, P.; Millet, J.; Theveniaux, J.; Barberousse, V. *Bioorg. Med. Chem. Lett.* **1998**, *8*, 1687-1688.
20. Renaut, P.; Millet, J.; Sepulchre, C.; Theveniaux, J.; Barberousse, V.; Jeanneret, V.; Vogel, P. *Helv. Chim. Acta* **1998**, *81*, 2043-2052.
21. Mani, K.; Havsmark, B.; Persson, S.; Kaneda, Y.; Yamamoto, H.; Sakurai, K.; Ashikari, S.; Habuchi, H.; Suzuki, S.; Kimata, K.; Malmstrom, A.; Westergren-Thorsson, G.; Fransson, L.-A. *Cancer Res.* **1998**, *58*, 1099-1104.
22. Malmberg, J.; Mani, K.; Saewen, E.; Wiren, A.; Ellervik, U. *Bioorg. Med. Chem.* **2006**, *14*, 6659-6665.
23. Whistler, R. L.; Es, T. V. *J. Org. Chem.* **1963**, *28*, 2303 2304.
24. Baudry, M.; Barberousse, V.; Collette, Y.; Descotes, G.; Pires, J.; Praly, J.-P.; Samreth, S. *Tetrahedron* **1998**, *54*, 13783-13792.

25. Collette, Y.; Ou, K.; Pires, J.; Baudry, M.; Descotes, G.; Praly, J. P.; Barberousse, V. *Carbohydr. Res.* **1999**, *318*, 162-166.
26. Skaanderup, P. R.; Poulsen, C. S.; Hyldtoft, L.; Jorgensen, M. R.; Madsen, R. *Synthesis* **2002**, 1721-1727.
27. Andresen, T. L.; Skytte, D. M.; Madsen, R. *Org. Biomol. Chem.* **2004**, *2*, 2951-2957.
28. Kornienko, A.; d'Alarcao, M. *Tetrahedron Lett.* **1997**, *38*, 6497-6500.
29. Kornienko, A.; d'Alarcao, M. *Tetrahedron Asymmetry* **1999**, *10*, 827-829.
30. Luchetti, G.; Ding, K.; d'Alarcao, M.; Kornienko, A. *Synthesis* **2008**, 3142-3147.
31. Siegbahn, A.; Aili, U.; Ochocinska, A.; Olofsson, M.; Roennols, J.; Mani, K.; Widmalm, G.; Ellervik, U. *Bioorg. Med. Chem.* **2011**, *19*, 4114-4126.
32. Haasnoot, C. A. G.; De Leeuw, F. A. A. M.; Altona, C. *Tetrahedron* **1980**, *36*, 2783-2792.
33. Tvaroska, I.; Mazeau, K.; Blanc-Muesser, M.; Lavaitte, S.; Driguez, H.; Taravel, F. R. *Carbohydr. Res.* **1992**, *229*, 225-231.
34. Saewen, E.; Massad, T.; Landersjoe, C.; Damberg, P.; Widmalm, G. *Org. Biomol. Chem.* **2010**, *8*, 3684-3695.
35. Neel, A. J.; Hilton, M. J.; Sigman, M. S.; Toste, F. D. *Nature (London, U. K.)* **2017**, *543*, 637-646.
36. Rubes, M.; Bludsky, O.; Nachtigall, P. *ChemPhysChem* **2008**, *9*, 1702-1708.
37. Oxford Diffraction (2006). *Crysalis CCD and Crysalis RED.* Oxford Diffraction Ltd, A., Oxfordshire, England.
38. Palatinus, L.; Chapuis, G. *J. Appl. Crystallogr.* **2007**, *40*, 786-790.
39. *CrystalMaker Software Ltd, O., England.*
40. Nishida, T.; Widmalm, G.; Sandor, P. *Magn. Reson. Chem.* **1995**, *33*, 596-599.
41. Nishida, T.; Widmalm, G.; Sandor, P. *Magn. Reson. Chem.* **1996**, *34*, 377-382.
42. Del Rio-Portilla, F.; Blechta, V.; Freeman, R. *J. Magn. Reson., Ser. A* **1994**, *111*, 132-135.
43. Pauli, G. F.; Chen, S.-N.; Lankin, D. C.; Bisson, J.; Case, R. J.; Chadwick, L. R.; Godecke, T.; Inui, T.; Krunic, A.; Jaki, B. U.; McAlpine, J. B.; Mo, S.; Napolitano, J. G.; Orjala, J.; Lehtivarjo, J.; Korhonen, S.-P.; Niemitz, M. *J. Nat. Prod.* **2014**, *77*, 1473-1487.
44. Navarro-Vazquez, A. *Magn. Reson. Chem.* **2012**, *50*, S73-S79.
45. Gaussian 09, Revision D.01, Frisch, M. J.; Trucks, G. W.; Schlegel, H. B.; Scuseria, G. E.; Robb, M. A.; Cheeseman, J. R.; Scalmani, G.; Barone, V.; Petersson, G. A.; Nakatsuji, H.; Li, X.; A. Marenich, M. Caricato,; Bloino, J.; Janesko, B. G.; Gomperts, R.; Mennucci, B.; Hratchian, H. P.; Ortiz, J. V.; Izmaylov, A. F.; Sonnenberg, J. L.; Williams-Young, D.; Ding, F.; Lipparini, F.; Egidi, F.; Goings, J.; Peng, B.; Petrone, A.; Henderson, T.; Ranasinghe, D.; Zakrzewski, V. G.; Gao, J.; Rega, N.; Zheng, G.; Liang, W.; Hada, M.; Ehara, M.; Toyota, K.; Fukuda, R.; Hasegawa, J.; Ishida, M.; Nakajima, T.; Honda, Y.; Kitao, O.; Nakai, H.; Vreven, T.; Throssell, K.; Montgomery, J. A. Jr.; Peralta, J. E.; Ogliaro, F.; Bearpark, M.; Heyd, J. J.; Brothers, E.; Kudin, K. N.; Staroverov, V. N.; Keith, T.; Kobayashi, R.; Normand, J.; Raghavachari, K.; Rendell, A.; Burant, J. C.; Iyengar, S. S.; Tomasi, J.; Cossi, M.; Millam, J. M.; Klene, M.; Adamo, C.; Cammi, R.; Ochterski, J. W.; Martin, R. L.; Morokuma, K.; Farkas, O.; Foresman, J. B.; J. Fox, and D.; Gaussian, Inc., Wallingford CT, 2016.
46. Becke, A. D. *J. Chem. Phys.* **1993**, *98*, 5648-5652.
47. Lee, C.; Yang, W.; Parr, R. G. *Phys. Rev. B Condens. Matter* **1988**, *37*, 785-789.
48. Wolinski, K.; Hinton, J. F.; Pulay, P. *J. Am. Chem. Soc.* **1990**, *112*, 8251-8260.
49. Cheeseman, J. R.; Trucks, G. W.; Keith, T. A.; Frisch, M. J. *J. Chem. Phys.* **1996**, *104*, 5497-5509.

50. Barone, V.; Cossi, M. *J. Phys. Chem. A* **1998**, *102*, 1995-2001.
51. Cossi, M.; Rega, N.; Scalmani, G.; Barone, V. *J. Comput. Chem.* **2003**, *24*, 669-681.
52. Deng, W.; Cheeseman, J. R.; Frisch, M. J. *J. Chem. Theory Comput.* **2006**, *2*, 1028-1037.
53. Lodewyk, M. W.; Siebert, M. R.; Tantillo, D. J. *Chem. Rev. (Washington, DC, U. S.)* **2012**, *112*, 1839-1862.